STRUCTURAL CONTROL AND HEALTH MONITORING
Struct. Control Health Monit. 2012; **19**:609–626
Published online 26 April 2011 in Wiley Online Library (wileyonlinelibrary.com). DOI: 10.1002/stc.458

Adaptive structural control using global vibration sensing and model updating based on local infrared imaging

Chun-Hung Lin[1,*,†,‡], Nebojsa Sebastijanovic[2,§], Henry T. Y. Yang[1,¶], Qi He[3,‡] and Xiaoyan Han[3,¶]

[1]*Department of Mechanical Engineering, University of California, Santa Barbara, CA 93106, U.S.A.*
[2]*ATA Engineering, Inc., El Segundo, CA 90245, U.S.A.*
[3]*Department of Electrical and Computer Engineering, Wayne State University, Detroit, MI 48202, U.S.A.*

SUMMARY

This paper presents a hybrid structural health monitoring system that was connected to an adaptive structural control algorithm to improve the control performance. The proposed vibration-based global damage detection method is combined with a local damage identification method using sonic infrared imaging. The numerical model and the monitor are updated for continuous structural monitoring and control during future earthquakes. The previously developed damage diagnosis technique is enhanced by including an equivalent simplified lumped-mass model deduced from a complex frame structure. Changes in global dynamic response characteristics due to damaged members or joints are first observed and the damage can be detected and located during the earthquake event. After the earthquake event, local damage is inspected in detail using sonic infrared imaging. The example of a three-story steel frame structure with a damaged column and a damaged joint is presented to demonstrate and evaluate the usefulness and effectiveness of the proposed concept. Results from numerical simulations indicate that the adaptive control strategy based on model updating improves the control performance.

Received 24 July 2010; Revised 31 January 2011; Accepted 25 February 2011

KEY WORDS: structural control; structural health monitoring; damage assessment; vibration; measurement feedback; nondestructive tests

1. INTRODUCTION

In the field of structural control, significant efforts have been devoted to protect civil infrastructures using various control strategies and devices, such as the passive and active structural control methods summarized by Soong and Costantinou [1]. Passive devices generally require no external energy source to serve their purpose as opposed to active devices that need external energy to apply forces to a structure. There are also semi-active control devices, known as hybrid devices, which combine passive and active devices and have the ability to offer the reliability of passive devices while keeping the versatility and adaptability of active devices. A survey paper addressing energy dissipation and different kinds of actuators is given by Housner *et al.* [2]. For more than two decades, researchers have investigated the possibility of using active and semi-active control methods to improve upon passive approaches for reducing structural responses [3].

*Correspondence to: Chun-Hung Lin, Department of Mechanical Engineering, University of California, Santa Barbara, CA 93106, U.S.A.
†E-mail: lin@engineering.ucsb.edu
‡Research Assistant.
§Project Engineer.
¶Professor.

One of the commonly used control design algorithms is based on linear quadratic regulator (LQR) theory [4], in which full states are needed. If only acceleration measurements are obtained for control, other states can be estimated using a Kalman filter [5,6], but an accurate model is required for this estimation process. This is known as linear-quadratic-Gaussian (LQG) control. However, most control strategies are based on structural models without the consideration for damage. The control performance can be improved by using adaptive control based on model updating. In this paper, a hybrid structural health monitoring method is proposed and used in the illustrative example to demonstrate the effectiveness of the proposed method.

Structural health monitoring methods can be generally categorized as global or local depending on the level of detail that the methods can provide regarding the condition of the structure. There are many methods that have been developed to globally determine whether there is damage in a structure. Most of them are based on changes in dynamic characteristics such as natural frequencies and mode shapes. Many of the global monitoring methods developed are summarized in surveys by Doebling *et al.* [7], Chang *et al.* [8], and Carden and Fanning [9]. The main disadvantage of global methods is that they cannot provide information on the location and severity of each damaged component. Global methods can only identify whether there is damage in the overall structure. Thus, it has been of interest to study structural health monitoring techniques that can detect and identify local damage or defects. The imaginable difficulty of such techniques is that these types of evaluations can be time consuming and expensive for complex structures so they are mainly used once the local region containing the damage is known. There are several techniques based on acoustic signals, electromagnetic field, radio frequency, optics, and others. Most of the recent non-destructive evaluation techniques have been summarized by Chang and Liu [10], including eddy current technique (effective for locating cracks), ultrasonic technique (for measuring the state of stress), magnetic flux leakage technique, X-ray technique, etc.

A global method for identifying and locating structural damage has been presented in previous studies [11,12]. The measured structural responses were assumed to be displacements, velocities, or accelerations. In the examples considered, the authors have shown that the developed algorithm was capable of detecting assumed damage based on the changes in dynamic responses and characteristics.

In the study of the present global damage detection algorithm, the previously developed global damage detection algorithm is enhanced by including an equivalent simplified lumped-mass model deduced from the complex high-rise frame structure. This enhanced technique can identify specific values for the floor masses and bending spring constants, whereas only parameters for state space representation of a simplified lumped-mass model were identified using the previous method [13].

In this study, the concept of combining the proposed global damage detection algorithm with the available local damage identification methods is considered and discussed. Once the proposed global damage detection algorithm has determined the condition of a structure based on the changes in dynamic responses and characteristics, local damage identification techniques can be used to provide more detailed and accurate assessment about the severity and extent of the damage. This can be performed after the earthquake is over since all local damage detection methods currently are based on the concept of active sensing. However, real time inspection and feedback would be preferred and advantageous but it would require a series of embedded interconnected sensors to collect data in real time. One of the main advantages of monitoring for damage in real time is that the structural model can be continuously updated so that an accurate model is readily available and can be used for structural control. In order to design an effective control system, it is important to have an accurate model that can be used to provide current information about the dynamic system in response to a particular earthquake input, especially when the system dynamics is changing due to damage.

Among all the available damage identification techniques, sonic infrared imaging technique has been developed and used for this study due to its ability to detect poor welds, cracks, or other defects that are invisible or only partially visible [14–17]. It is a novel non-destructive evaluation technology that overcomes many drawbacks of traditional non-destructive evaluation techniques. It is an effective, fast, and wide-area non-destructive evaluation method. Sonic infrared imaging combines acoustic excitation and infrared sensing technologies for local damage and defect detection. This technique employs a pulse of ultrasound/sound excitation to cause self heating in

DOI: 10.1002/stc

damaged/defect areas, which results in the rise of infrared (thermal) radiation from the damaged/defect areas and their surroundings. Infrared sensors are used to image the thermal radiation from the target. The damaged/defect areas can be identified from the changes in thermal radiation in the infrared images. The location of the damage/defects can be accurately identified and the severity of the damage can be evaluated at the same time as well.

The progress on combing a hybrid structural health monitoring system with an adaptive control system is illustrated through a three story model with local defect of a column with channel cross section and a damaged joint. Once the existence of damage is indicated through the global damage detection algorithm, sonic infrared imaging can be used immediately and quickly for detecting and evaluating local damage. Based on the results of the hybrid structural health monitoring system, local members can be updated with new bending stiffness of a beam or column or rotational stiffness of a joint to instantly update the global structural model. Thus, new local or perhaps smaller damage can be located by this continuously updating method in real time. The control strategy can be modified at that time as well. The concept of combing the global sensing and local infrared imaging, where the global sensing is used to predict the existence of damage in a structure, and infrared imaging is used for local damage identification and evaluation, is shown in Figure 1. In addition to its ability to detect invisible or partially visible defects, sonic infrared imaging technique has the potential of being used remotely,

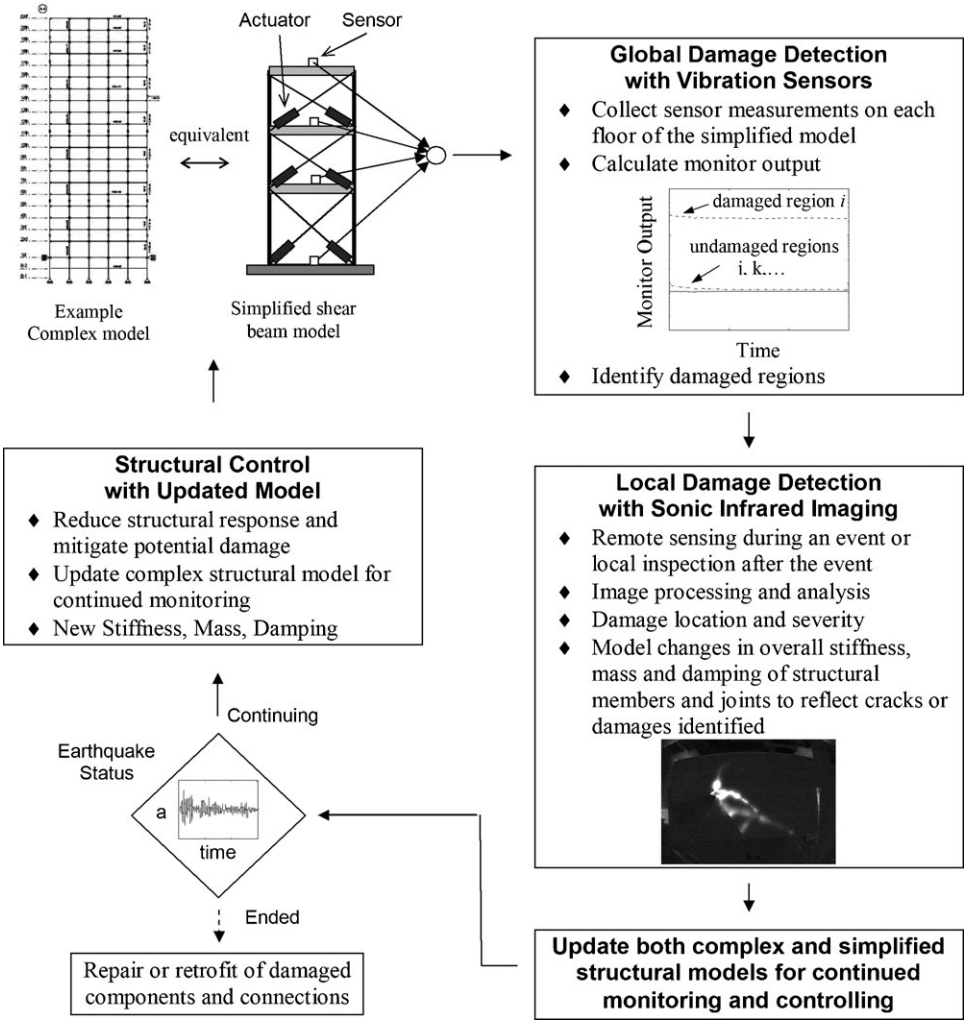

Figure 1. Schematic diagram of the hybrid structural health monitoring and control system combining global sensing and local sonic infrared imaging.

DOI: 10.1002/stc

i.e. without the need for local active sensing, and remote sensing could potentially be used to identify damaged components and joints. The use of such remote sensing system in real time may become reality in the near future. With such expectations and assumptions, the development of a hybrid structural health monitoring system that can be implemented for real time structural health monitoring is illustrated in this paper conceptually, although for the most part realistically.

2. GLOBAL DETECTION OF DAMAGE

The global damage diagnosis algorithm presented in previous studies [11,12,18] uses one of the three kinds of measurements, displacements, velocities, or accelerations, as inputs. For the purpose of simplicity, displacement feedback is used in this study. By decoupling the stiffness of each floor, monitors are designed to detect damage of each floor separately for a lumped-mass model. This makes it possible to identify damaged regions, but does not provide detailed local damage information such as cracks in structural members, welding, joints, etc. In this study, a system identification method is proposed and used to enhance the previous damage detection method and enable the detection of damage in a complex frame structure.

2.1. System identification technique

The previously developed damage detection method [11] has been improved by including a system identification technique. This technique can identify an equivalent simplified lumped-mass model deduced from a complex high-rise frame structure and can be used in the damage diagnosis algorithm. The concept of coordinate transformation with mode shapes and modal matrix [19] is utilized as well.

First, natural frequencies and mode shapes can be obtained by implementing the finite element frame-based model. The jth mode shape, which corresponds to the desired degree of freedom, is selected and defined as Φ_j. The orthonormal modal matrix Φ for the n-degree-of-freedom system can be written as

$$\mathbf{\Phi} = [\,\phi_1 \quad \phi_2 \quad \ldots \quad \phi_j \quad \ldots \quad \phi_n\,] \tag{1}$$

Second, the mass of ith floor of the simplified lumped-mass model, m_i, can be obtained by adding up the mass of every member of the finite element frame-based model for each floor, i.e. the mass of each story is divided in half and lumped at the column-beam joint. The modal stiffness k_{jj} and modal damping c_{jj} can be calculated as

$$k_{jj} = \omega_j^2 \tag{2}$$

$$c_{jj} = 2\xi_j\omega_j \tag{3}$$

where ω_j is the natural frequency and ζ_j represents the damping ratio of the jth mode.

Then, the mass, damping, and stiffness matrices of the simplified model can be determined by coordinate transformation and denoted as M, C, and K, respectively.

$$\mathbf{M} = \mathrm{diag}[m_i] \tag{4}$$

$$\mathbf{C} = \mathbf{\Phi}^{-\mathrm{T}}\mathrm{diag}[c_{jj}]\mathbf{\Phi}^{-1} \tag{5}$$

$$\mathbf{K} = \mathbf{\Phi}^{-\mathrm{T}}\mathrm{diag}[k_{jj}]\mathbf{\Phi}^{-1} \tag{6}$$

The governing equation of the simplified lumped-mass model under external excitations can now be constructed as

$$\mathbf{M}\ddot{z}+\mathbf{C}\dot{z}+\mathbf{K}z = \mathbf{F}(t) \tag{7}$$

where z is the displacement vector and $\mathbf{F}(t)$ is the time-dependent external force.

Two examples presented in the previous study [13] are considered to demonstrate the effectiveness of the model simplifying technique. In both examples, North–South component of acceleration of the 1940 El Centro earthquake is used as the excitation.

DOI: 10.1002/stc

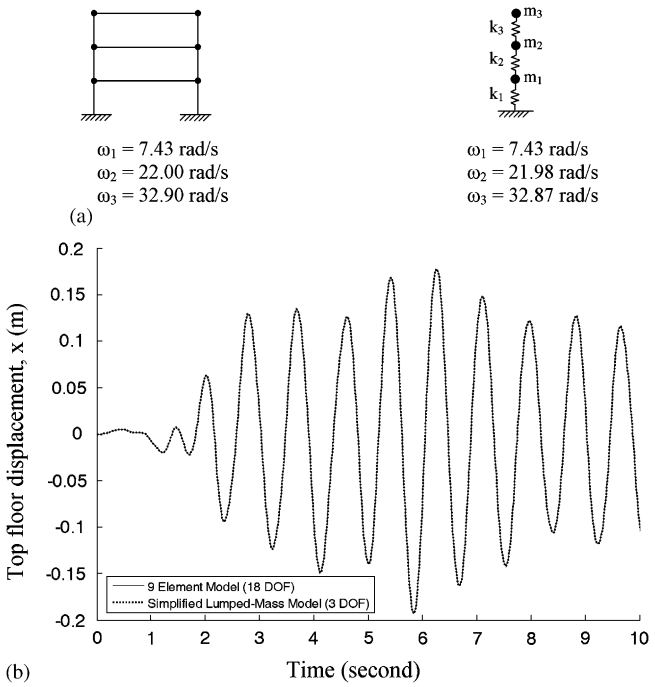

Figure 2. Identification of masses and stiffness for the simplified 3-dof lumped mass model of a 3-story frame structure: (a) frequency comparison and (b) response comparison.

The first example is a single bay, three-story frame model, which was first illustrated as an example in the text by Biggs [20]. It has been simplified into a three degree-of-freedom lumped-mass model ($m_1 = 25\,001$ kg, $m_2 = 23\,290$ kg, $m_3 = 11\,695$ kg; $k_1 = 4936$ kN/m, $k_2 = 7287$ kN/m, $k_3 = 6498$ kN/m), as shown in Figure 2. It can be observed that natural frequencies and structural responses are almost identical for the nine element frame model and the three degree-of-freedom simplified lumped-mass model.

The second example is the 284 element model benchmark proposed by Spencer *et al.* [21], which has been simplified into a four degree-of-freedom lumped-mass model ($m_1 = 60\,000$ kg, $m_2 = 58\,000$ kg, $m_3 = 58\,000$ kg, $m_4 = 22\,000$ kg; $k_1 = 1279$ kN/m, $k_2 = 2270$ kN/m, $k_3 = 1706$ kN/m, $k_4 = 801$ kN/m), as illustrated in Figure 3. Once again, natural frequencies and structural responses are almost identical. For each example, it is shown that, in addition to matching frequencies and structural responses, the present technique also identifies specific values for the mass and stiffness of each floor, whereas only parameters of the transfer function and state space representation of a lumped-mass model can be identified using the previous method [13]. Thus, this enhanced system identification technique may be used to identify a simplified lumped-mass model for a complex frame model.

2.2. Detecting stiffness reduction in connections and joints

In structural analysis, it is a common practice to assume that joints are perfectly rigid for steel and reinforced concrete frame structures. However, in actual structures, typical joints and connections do not behave in a perfectly rigid manner. When analyzing a structure, it is common to use semi-rigid connections to develop a more realistic structural model and achieve more accurate analysis. Accurate description of the true behavior of connections falls within the entire flexibility spectrum, from rigid connections (fixed) to semi-rigid connections to flexible connections (pinned) [22,23]. Some typical configurations of beam-column connections in steel frames [24] are shown in Figure 4(a) while the categorization of joints based on the moment-curvature characteristics corresponding to those configurations is shown in Figure 4(b). In order to develop an accurate structural model, it is necessary to determine the actual stiffness of

DOI: 10.1002/stc

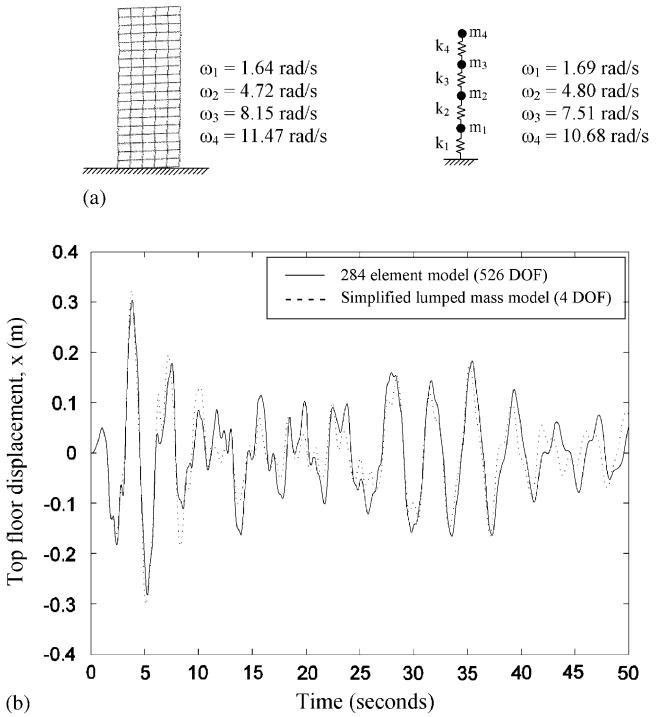

Figure 3. Identification of masses and stiffness for the simplified 4-dof lumped mass model of a benchmark structure: (a) frequency comparison and (b) response comparison.

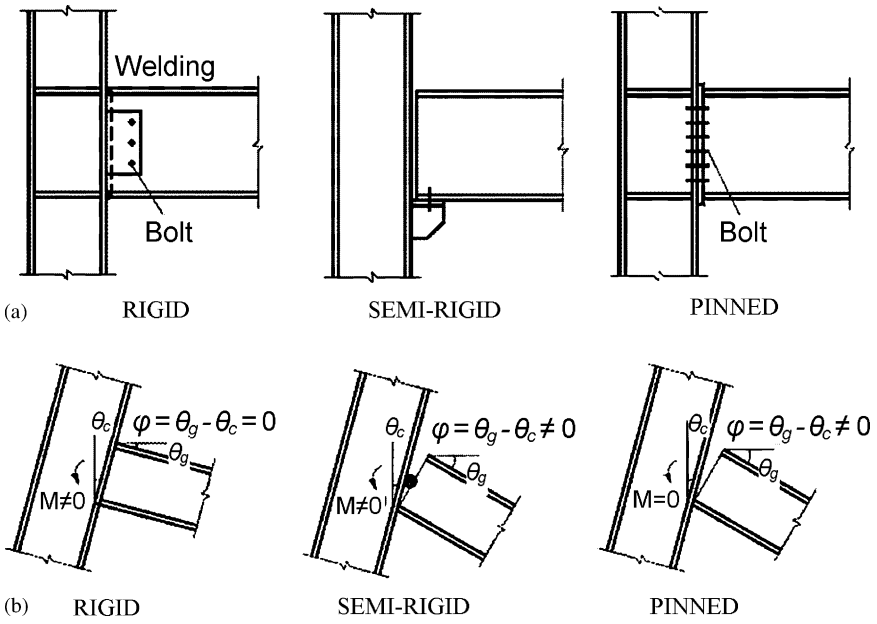

Figure 4. (a) Some typical configurations of beam-column connections in steel frames and (b) moment and rotations of beam-column connections (g, girder; c, column).

connections in a structure. In previous studies [11,12], joints were modeled as perfectly rigid and detecting changes in joint stiffness was not considered. Only changes in floor stiffness that occurred due to assumed damage to structural members were considered. However, it seems logical to investigate the possibility of using the proposed structural health monitoring system

DOI: 10.1002/stc

for detecting changes in rotational stiffness for both fully and partially rigid joints and connections due to damage, missing parts, imperfections, etc. Such changes in rotational stiffness can occur due to damage caused by external disturbances, such as earthquakes, strong winds, and impact, or even due to manufacturing or construction defects. In this preliminary study, the concept of detecting changes in rigidity or flexibility of joints using the proposed global damage detection method is illustrated using a one-story frame structure analyzed by Lui and Chen [25], with properties as shown in Figure 5(a). The one-story frame was modeled using three, six, and nine beam elements, respectively, while almost identical natural frequency and structural response was obtained. An equivalent lumped-mass model ($m = 652\,\text{kg}$, $k = 8.6 \times 10^6\,\text{N/m}$) shown in Figure 5(b) was developed using the system identification algorithm described in the previous section. Due to the assumption of inextensibility, it is assumed that each of the two joints has only three degrees of freedom. Thus, for joint 2, the three degrees of freedom are: horizontal deflection u, rotation or slope θ_{21} of column 2-1, and rotation or slope θ_{23} of beam 2-3. It should be noted that joints 2 and 3 are modeled using rotational springs to include the effect of joint flexibility. The natural frequency of the one-story frame structure based on the flexibility of joint 2 is shown in Figure 6. Fixity factor γ [26] and multiplication factor $\grave{\imath}$ [27] have been used in previous studies to classify connection types according to Eurocode 3 (1993), as shown in Table I. It can be seen that by using a perfectly rigid joint 2, the natural frequency is $\omega = 114.8\,\text{rad/s}$ while $\omega = 90.6\,\text{rad/s}$ if joint 2 is pinned. This indicates a 21% variation in natural frequency and the range between these two frequencies

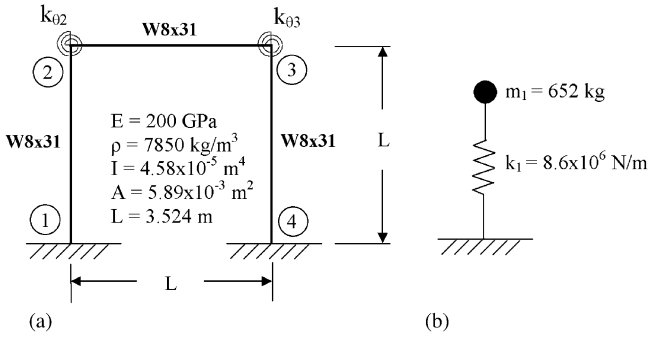

Figure 5. (a) Three element modeling of the one-story frame structure and (b) equivalent simplified single degree-of-freedom lumped mass model.

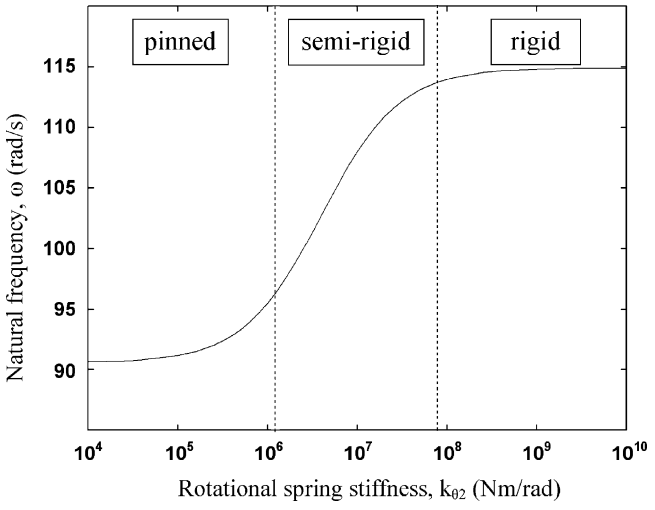

Figure 6. Natural frequency of the one-story frame structure.

DOI: 10.1002/stc

Table I. Classification of connections for unbraced frame structures as defined in Eurocode 3.

	Pinned connection	Semi-rigid connection	Rigid connection
Multiplication factor	$0 \leqslant \mu < 0.5$	$0.5 \leqslant \mu \leqslant 25$	$25 < \mu < \infty$
Fixity factor	$0 \leqslant \gamma < 0.143$	$0.143 \leqslant \gamma \leqslant 0.891$	$0.891 < \gamma \leqslant 1$

Note: Multiplication factor [27], $\mu = k_{\theta 2}/(EI/L)$ Fixity factor [26], $\gamma = 1/1+(3EI/L/k_{\theta 2})$ where EI/L is the flexural rigidity of a beam and $k_{\theta 2}$ is the rotational spring stiffness.

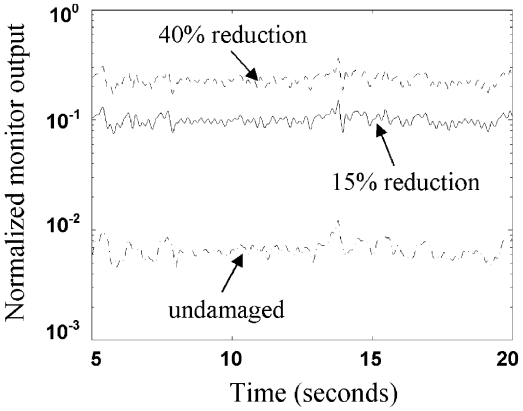

Figure 7. Detecting the reduced stiffness of rigid joint 2 in the one-story frame model using acceleration feedback.

represents a connection that exhibits a semi-rigid behavior. The model is excited by the N-S component of acceleration of the 1940 El Centro earthquake and the measured structural response is assumed to be acceleration at the first floor. The proposed damage detection algorithm can be used to determine whether a joint has lost its rigidity by monitoring the equivalent lumped-mass model. The ability of the proposed damage detection algorithm to detect changes in the flexibility of joint 2 using acceleration feedback is shown in Figure 7. Different values of α represent the degree of rotational stiffness reduction due to damage for joint 2, i.e. $\alpha = 0\%$ for the undamaged joint while $\alpha = 15\%$ indicates a 15% reduction in rotational stiffness due to joint damage. It can be observed in the figure that monitor output results for undamaged and damaged rigid joint are easily distinguished by the obvious separation of the curves.

3. LOCAL SONIC INFRARED IMAGING

Sonic infrared imaging is a novel non-destructive evaluation technology that combines acoustic excitation and infrared sensing methods to overcome many drawbacks of traditional non-destructive evaluation techniques. The main advantage is in its versatility and ability to detect defects in different materials and structures, including poor bonding in welded or brazed joints, open or fatigue cracks, or other defects that are invisible or only partially visible [14–17]. It is important to note that the accuracy of the semi-rigid frame design is determined by the accuracy of the joint parameters, as shown by Wald [28]. The prediction of joint parameters is affected by joint imperfections, e.g. lack of fit, bolt holes' sizes, position variation, tightening differences, and even cracks. For simplicity, the practically important and complex problem of determining the percentage reductions of rotational stiffness in a joint due to various scenarios of joint damage has not been investigated in this preliminary study; only the effect of assumed reduction in rotational stiffness of the joint has been considered in order to determine the effectiveness of the proposed global damage detection algorithm. It should be noted that a similar approach can be used to determine changes in joint stiffness for semi-rigid connections. It would be of interest to further investigate the limitations of the proposed algorithm in terms of its sensitivity to rotational stiffness reduction of joints as well as its ability to distinguish

DOI: 10.1002/stc

between beam or column member and joint damage. This would include examples of multi-story frames along with practical assessments of percentage reduction of rotational stiffness due to joint damage and reduction of bending stiffness due to beam or column damage under various practical damage scenarios.

3.1. Determining stiffness reduction in columns and beams

The assumed damage due to an open crack was modeled as an 18% reduction of the moment of inertia in one column of the first floor. The formulation for modeling variation in beam stiffness due to damage follows the study by Sinha *et al*. [29] which was based on the concept presented by Christides and Barr [30]. The general approach can be seen in Figure 8 where the beam with a crack is shown in Figure 8(a) while the resulting variation in bending stiffness of the column is shown in Figure 8(b).

Schematic drawing of using the sonic infrared imaging technique for local damage detection of a steel C channel of the 1st floor column is shown in Figure 9. Ultrasonic or acoustic waves are injected by the transducer to cause heating in damaged area/defects, and an infrared camera is used to image the structure to locate the damage for evaluation. The structural elements can be scanned in sections whose size would depend on the infrared camera resolution until the exact location and severity is determined. It is assumed that all selected sections along the beam have been scanned and cracks were discovered in the top beam. Therefore, only the damaged segment

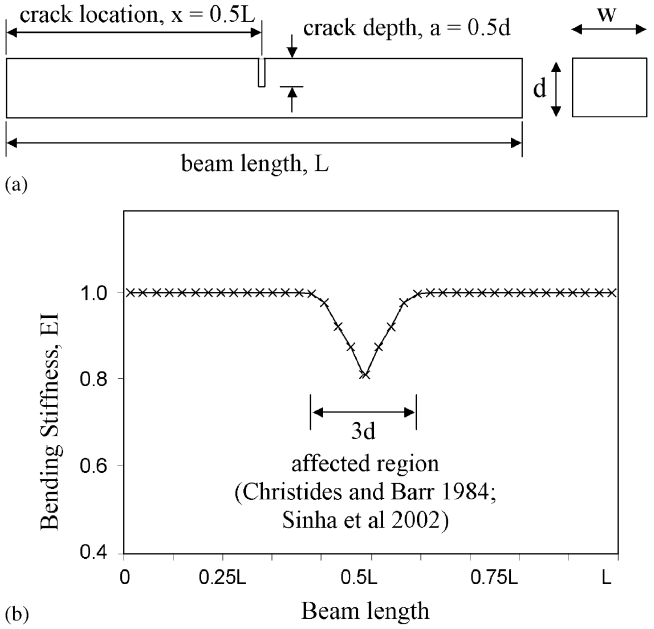

Figure 8. (a) Damaged beam with an open crack and (b) bending stiffness variation due to the assumed crack.

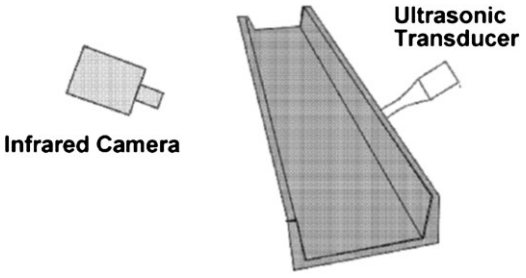

Figure 9. Schematic drawing of sonic infrared imaging for local damage detection.

DOI: 10.1002/stc

of the C channel is presented and analyzed. For the segment considered, the excitation source is 15 kHz, the focal plane array of the infrared camera has 640×512 infrared detectors which can come up with 85 frames per second, and the infrared sensors are sensitive to mid-wavelength infrared, in the range of 2–5 μm. The C channel section is 33 in. deep, 5 in. wide, and 1.75 in. thick, with flange width of 1.5 in. and the thickness of the steel walls is about one quarter of an inch, as shown in Figure 10 (AISC $C5 \times 6.7$). It is obvious that a structure of this size can be imaged as a whole and the infrared image will still have sufficient spatial resolution to identify the damage in the structure. Interior cracks in the C channel were created through thermal fatigue with external impact to simulate the damage. In Figure 11, infrared images of both

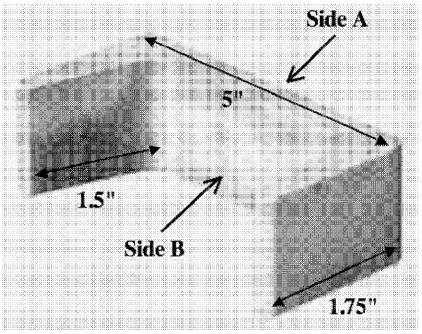

Figure 10. Steel C channel section with dimensions.

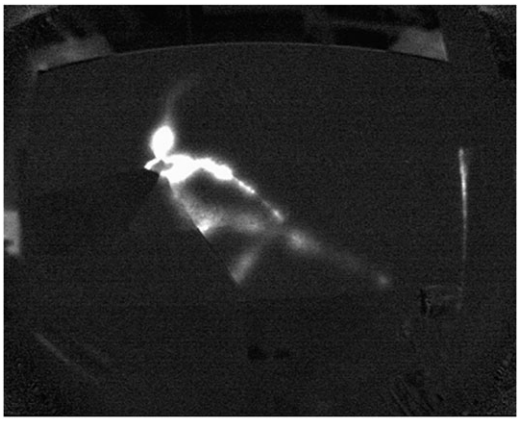

Side A

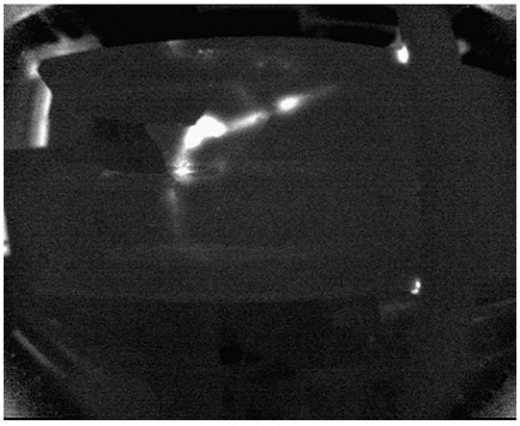

Side B

Figure 11. Sonic infrared images indicating cracks.

DOI: 10.1002/stc

side A and side B clearly show the embedded damage, which appear to be bright in the images. Crack dimensions that were discovered during local infrared inspection are shown in Figure 12(a). It can be seen that there are quite a few interconnected cracks along the beam segment considered. For simplicity, a rough approximation of the damaged area is described by an opening, as shown in Figure 12(b). For the lack of a more detailed modeling of these cracks with accurate theory and approximations for the distribution of the moment of inertia (I) through the length of the beam, a rough approximation method is proposed for simplicity. The moment of inertia has been approximated at ten cross sections along the beam length as indicated by I_i in Figure 12(b). Based on this approximation, an estimate of the variation in moment of inertia is shown in Figure 12(c) so as to roughly illustrate the proposed concept although rigorous theory and approximation method have yet to be developed. In order to use the global damage detection algorithm, the damaged beam on the third floor was represented by an equivalent beam with its 'effective' moment of inertia determined using the approach presented by Chehil and Jategaonkar [31]. In that study, the authors used the concept of effective moment of inertia to develop a method for estimating natural frequencies of beams with linear inertia variation in a non-continuous manner. It was shown that the effective moment of inertia can be calculated using the expression

$$I_{\text{eff}} = I_0 \pm i\left[\frac{1}{4} + \frac{1}{2n^2\pi^2}(1 - \cos n\pi)\right] \tag{8}$$

which simplifies to $I_{\text{eff}} = I_0 + i/4$ as $n \to \infty$, where n is the number of modes, I_0 is the moment of inertia of the undamaged beam, and i represents the variation in moment of inertia along the

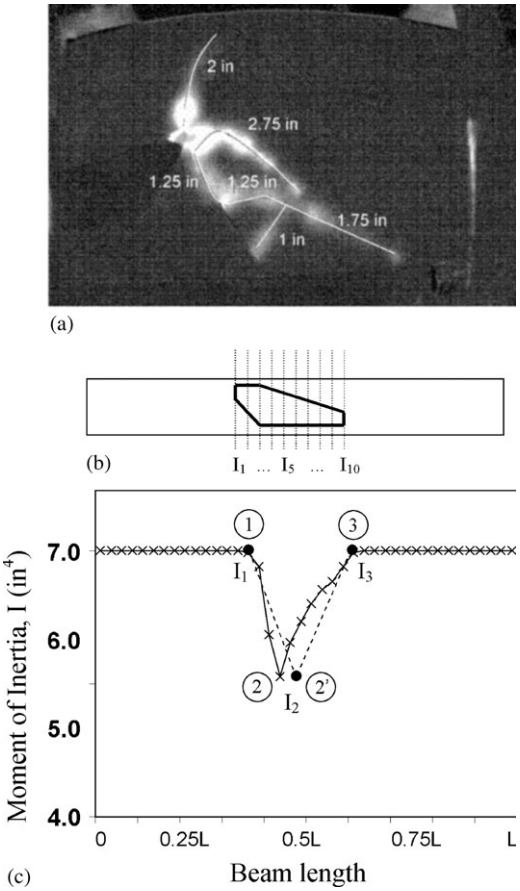

Figure 12. (a) Dimensions of cracks found in the steel C channel, side A; (b) rough approximation of the damaged segment due to cracks; and (c) variation in moment of inertia along the beam due to approximated damage.

DOI: 10.1002/stc

beam, i.e. rate of change in the moment of inertia multiplied by I_0. Mathematically speaking, $i = (\partial I/\partial x)I_0$.

Considering the beam shown in Figure 13, $i = (I_2 - I_1)/\Delta L = (5.58–7.03)/(2) = -0.725 \times I_0$ from point 1 to point 2 and $i = (I_3 - I_2)/\Delta L = (7.03–5.58)/(2) = 0.725 \times I_0$ from point 2 to point 3. For simplicity, it is assumed that the moment of inertia linearly reduces from point 1 to point 2 and linearly increases from point 2 to point 3. It should also be noted that because the approximation suggested by Chehil and Jategaonkar [31] is based on the assumption that the moment of inertia curve is symmetrical, the valley of the actual curve 1-2-3 representing the reduction of moment of inertia is slightly shifted to the right to become a symmetrical V-shaped curve 1-2′-3. Therefore, the reduction in the moment of inertia of the C channel based on the estimated dimensions of the cracked zone over the damaged channel segment would result in the effective moment of inertia of $I_{\text{eff}} = 0.82 \times I_0$. This indicates an 18% stiffness reduction in the first floor column of the frame model shown in Figure 14, which can be identified by the global damage detection algorithm, as shown in Figure 15. This damage is equivalent to a 9% stiffness reduction in the first floor of the simplified lumped-mass model (Figure 14(b)). Damaged and undamaged outputs are clearly distinguished by a jump in the value of the normalized monitor output. Detected changes in certain structural parameters of damaged members or joints can be used to update the existing structural model for continued monitoring during the earthquake event. Only those critical members and joints that are potentially vulnerable to occurrence of damage would need to be identified and monitored in real time. Based on the concept presented, it seems that a hybrid structural health monitoring system could be developed by combining the method for global damage detection and a method for

(a)

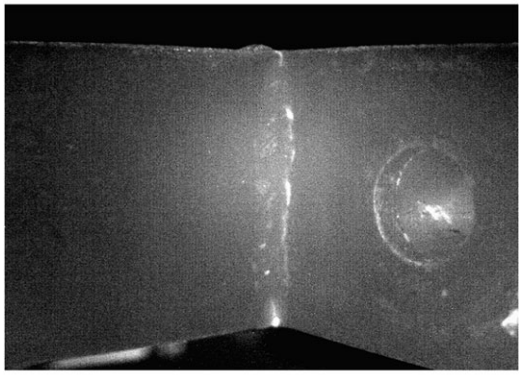

(b)

Figure 13. (a) Optical image of the welded joint, where the beam is 7.5 cm (3″) thick and (b) sonic infrared image of the joint showing subsurface cracks along the joint.

DOI: 10.1002/stc

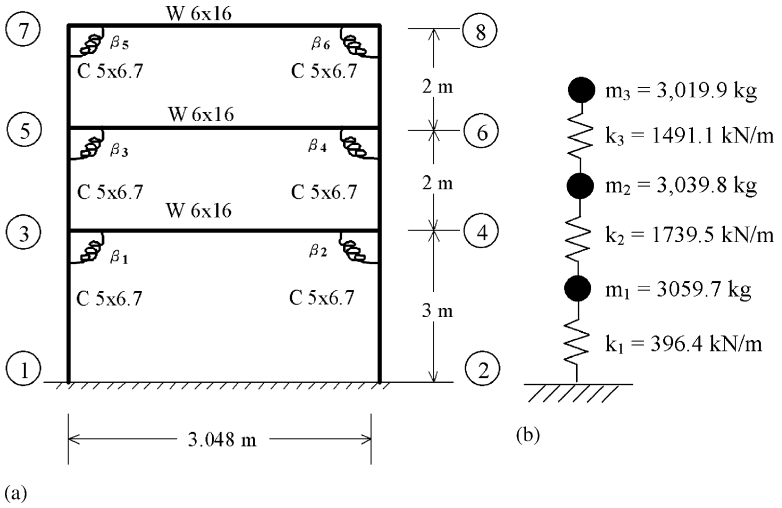

Figure 14. (a) Three-story frame model and (b) equivalent simplified 3 degree-of-freedom lumped-mass model.

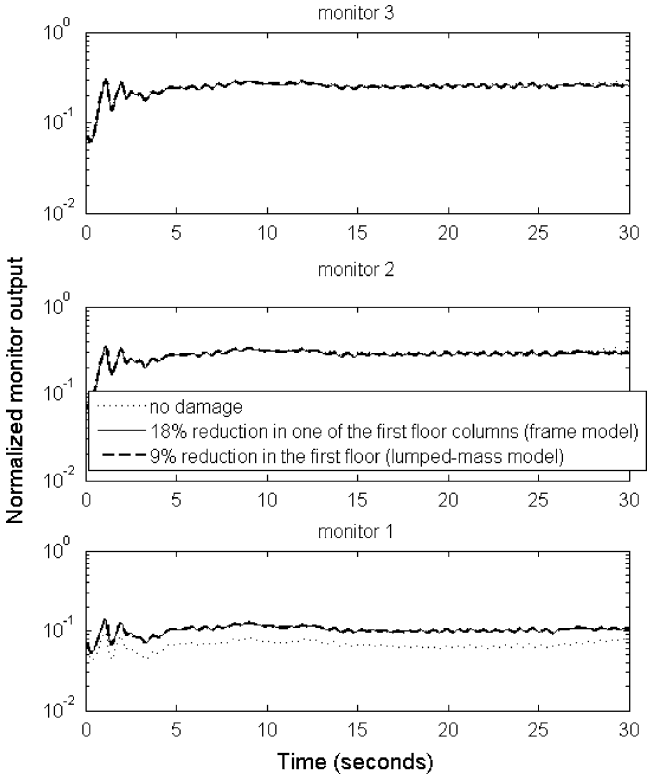

Figure 15. Damage detection for the three-story steel frame model using displacement feedback and assuming 18% stiffness reduction in one column of the first floor.

local damage identification so that both the exact location of the damage and its degree of severity can be determined in real time.

3.2. Determining stiffness reduction in connections and joints

For the example considered, once the changes in joint flexibility have been determined using the proposed global damage detection algorithm, local damage identification methods can be used

DOI: 10.1002/stc

to find damaged or failed joints. Figure 13 shows an example of applying sonic infrared imaging technique on a damaged joint with cracks along the welded edge.

4. ILLUSTRATIVE EXAMPLE

The example of a single bay, three-story frame model considered in the text by Biggs [20] is modified by changing all columns to C5 × 6.7 and all beams to W6 × 16 as shown in Figure 14(a). The reason for this change to a channel beam is due to the availability of such a beam and the practical simplicity for experimental creation and detection of embedded cracks of such a specimen in the present laboratory. The structural members have the following properties with reference to AISC Manual of Steel Construction (1992):

Young's Modulus	$E = 200$ GPa
Density	$\rho = 7.83 \times 10^3$ kg/m^3

For column elements,

$$C5 \times 6.7, \quad I = 3.12 \times 10^{-6} \text{ m}^4, \quad A = 1.27 \times 10^{-3} \text{ m}^2$$

For beam elements,

$$W6 \times 16, \quad I = 1.34 \times 10^{-5} \text{ m}^4, \quad A = 3.06 \times 10^{-3} \text{ m}^2$$

Additional masses are added to the beam elements in order to model the mass of the floors that would be supported by the frame:

$$M_1 = 3000 \text{ kg}, \quad M_2 = 3000 \text{ kg}, \quad M_3 = 3000 \text{ kg}$$

The frame is modeled using beam and column elements with two degrees of freedom at each joint, i.e. horizontal displacement and rotation. System identification technique described in the previous section is used to identify an equivalent simplified lumped-mass model shown in Figure 14(b) that can be used in the global damage detection algorithm. The frequencies for the first three modes are identified to be $\omega_1 = 6.35$ rad/s, $\omega_2 = 22.69$ rad/s, $\omega_3 = 40.91$ rad/s, respectively.

The frame model is excited by the N-S component of acceleration of the 1940 El Centro earthquake and displacements are measured at each floor. The concept of applying adaptive structural control using global vibration sensing and model updating based on local sonic infrared imaging is explored on this single bay, three-story test frame model shown in Figure 14(a).

Global damage detection is assumed to be performed in real time in this study and monitors directly utilize structural response measurements in the time domain. Once the existence of damage has been determined using the proposed global damage detection algorithm, in this case in the first floor column and then the third floor joint, sonic infrared imaging is proposed to investigate the damage locally. The model updating is based on the detailed information provided by both the global and local damage detection methods. The updated model, which includes information about the damage, is then used to improve the control performance. Even though global damage detection can only identify a general location of the damage, i.e. a damaged floor, it is still useful since sonic infrared imaging can focus on a smaller region and reduce the delay in feedback real time required to locate damaged members. Currently, sonic infrared imaging can only be used after the earthquake has ended to detect local damage so that it can be inspected in detail for the purpose of repair and retrofit. However, sonic infrared imaging technique has the potential of being used remotely and the current study is based on the premise and expectation that the use of such remote sensing in real time will become reality in the near future.

4.1. Detecting damage in a three-story structure with damaged beam and damaged joint

The following example is presented here to test the ability of the proposed damage detection method.

First, a crack is assumed to occur in the column between joint 1 and joint 3 as shown in Figure 14(a), and the equivalent moment of inertia is reduced by 18%. The global damage detection method is used and damage is detected on the first floor. Monitor 1 indicates that k_1 is

DOI: 10.1002/stc

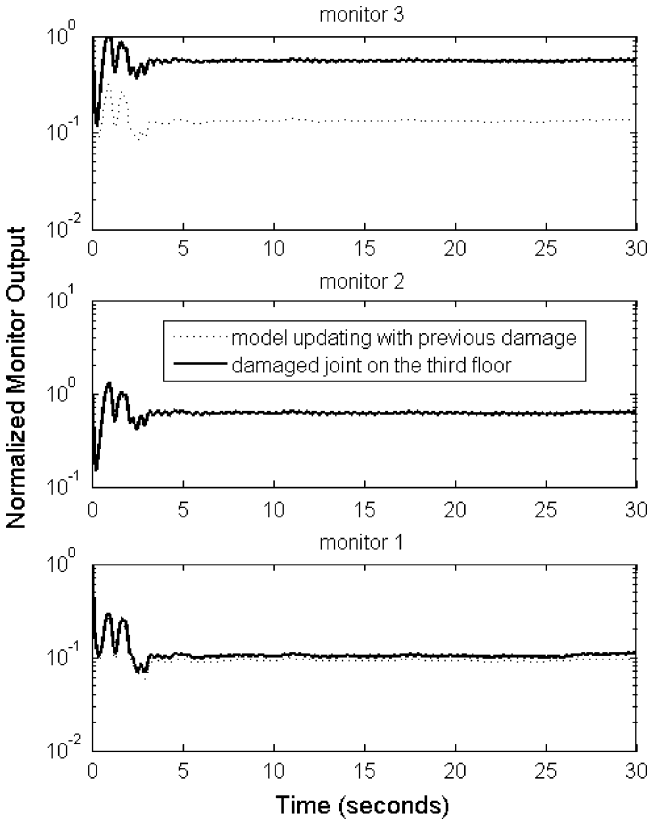

Figure 16. Damage detection for the three-story steel frame model using displacement feedback and assuming stiffness reduction in one joint of the third floor.

decreased by 9% (Figure 15). After the damage is located, the sonic infrared imaging local damage detection method is then used to discover the crack. The equivalent moment of inertia of the damaged column is calculated and shown to be decreased by 18% using the method described in Section 3.1. Based on this information, the frame model is updated and the parameters in the global damage diagnosis algorithms are recalculated using the system identification technique. Then, a new crack is assumed to occur in joint 8 as shown in Figure 13. The joint, assumed to be damaged, becomes semi-rigid. The rotational stiffness β_6 in Figure 14(a) is thus assumed to be reduced to 10^7 N m/rad (for rigid joint, it was assumed to be 10^{11} N m/rad). The global damage detection method is used and the new damage is detected on the third floor (Figure 16). Finally, the crack in joint 8 can be found by implementing the local damage detection method. The process can be continued to monitor for any new damage.

4.2. Adaptive structural control with model updating

Considering another example, it is assumed that the column on the first floor and joint on the third floor are both damaged, and this damage causes a 20% stiffness reduction in the first floor stiffness (k_1) and 30% stiffness reduction in the third floor stiffness (k_3). This information can be fed back to the computational model, updating the model for continuous structural health monitoring and adaptive control.

In this example, the structure is controlled by an ideal active tendon on the first floor using LQG active control algorithm, which minimizes the cost function $J = 2.07 \times 10^3 \ddot{x}_3^2 + 6.2 \times 10^9 x_1^2 + f_1^2$. The acceleration response of the structure is measured at each floor, and a Kalman filter is designed to estimate the required states, which are the displacements and velocities. Since Kalman filters depend on an accurate model in order to estimate the full states, the model updating technique has a potential to achieve better control performance. The N-S

DOI: 10.1002/stc

Table II. Comparisons of peak responses with and without updated model for frame model with damaged column on the first and third floors.

	Uncontrolled	LQG optimal control without model updating	LQG optimal control with model updating	Percentage of improvement due to model updating (%)
Displacement (cm)				
x_1	14.996	11.959	7.325	38.75
x_2	16.861	13.550	8.339	38.46
x_3	18.496	15.002	9.294	38.05
Drift (cm)				
d_1	14.996	11.959	7.325	38.75
d_2	1.880	1.636	1.066	34.84
d_3	1.661	1.452	1.116	23.11
Acceleration (cm/s^2)				
a_1	499	380	300	20.94
a_2	520	444	297	33.04
a_3	574	502	386	23.11
Max force (N)				
f	0	6672	6086	8.79

acceleration component of the 1940 El Centro earthquake is used as the external excitation in the simulation. Peak responses of the three-story frame model with and without model updating are shown in Table II. Peak displacements are reduced by 38–39% when using adaptive control with model updating. First floor drift is reduced by 38.75% and second floor acceleration is reduced by 33.04%.

5. CONCLUSIONS

In this study, the previously presented global damage detection algorithm using displacement, velocity, or acceleration measurements as feedback has been improved by including a system identification capability. This enables monitoring of complex structures by identifying an equivalent simplified lumped-mass model with specific values for floor mass and bending stiffness. Two examples, including a three-story steel frame model and a benchmark model, were presented to illustrate the effectiveness of the improved system identification technique.

The global damage detection algorithm was then evaluated using a single-story steel frame structure with assumed changes in rotational stiffness of the joint, and a three-story steel frame model with a damaged column and joint. For the examples presented, it was shown that the proposed global damage detection algorithm can detect stiffness changes due to assumed (or actual) damage, as well as changes in joint stiffness.

The concept of combining the global damage detection algorithm and local infrared imaging technique in order to develop a hybrid structural health-monitoring system has been presented and discussed as well. This concept is illustrated using a three-story steel frame building with a local damage of a column with channel cross section. Damage to the column is approximated based on the experimental results. Once changes in stiffness due to the assumed damage are indicated by the global damage detection algorithm, sonic infrared imaging technique is used to detect and evaluate local damage more accurately. Sonic infrared imaging technique has been developed and used for this study due to its ability to detect poor welds, cracks, or other defects that are invisible or only partially visible. It also seems that its potential of remote monitoring could be used for real time structural health monitoring once the necessary technology for real time passive sensing is developed. Currently, the proposed concept may be quite useful after the earthquake has ended. Once the global damage detection identifies a general location of the damage, sonic infrared imaging can focus on a smaller region and reduce the time required to locate damaged members, so they can be inspected in detail for the purpose of repair and retrofit.

DOI: 10.1002/stc

For the adaptive control using model updating, it is noted that if the updated model with damage information is considered in the calculation of the Kalman estimation and LQR control gain, the control performance can be significantly improved.

ACKNOWLEDGEMENTS

This study is sponsored by the National Science Foundation grant CMS 0511046. The guidance of program director, Dr S. C. Liu, is gratefully acknowledged. Valuable discussions with Tian-Wei Ma are acknowledged.

REFERENCES

1. Soong TT, Costantinou MC. *Passive and Active Structural Vibration Control in Civil Engineering*. Springer: New York, 1994.
2. Housner GW, Bergman LA, Caughey TK, Chassiakos AG, Claus RO, Masri SF, Skelton RE, Soong TT, Spencer BF, Yao JTP. Structural control: past, present, and future. *Journal of Engineering Mechanics* (ASCE) 1997; **123**(9):897–971. DOI: 10.1061/(ASCE)0733-9399(1997)123:9(897).
3. Spencer Jr BF, Nagarajaiah S. State of the art of structural control. *Journal of Structural Engineering* 2003; **129**(7):845–856.
4. Kwakernaak H, Sivan R. *Linear Optimal Control Systems*. Wiley-Interscience: New York, 1972.
5. Dyke SJ, Spencer Jr BF, Quast P, Sain MK, Kaspari Jr DC, Soong TT. Acceleration feedback control of MDOF structures. *Journal of Engineering Mechanics* (ASCE) 1996; **122**(9):907–918. DOI: 10.1061/(ASCE)0733-9399(1996)122:9(907).
6. Spencer BF, Sain MK, Won CH, Kaspari DC, Sain PM. Reliability-based measures of structural control robustness. *Structural Safety* 1994; **15**(1–2):111–129. DOI: 10.1016/0167-4730(94)90055-8.
7. Doebling SW, Farrar CR, Prime MB, Shevitz DW. Damage identification and health monitoring of structural and mechanical systems from changes in their vibration characteristics: a literature review. *LA-13070-MS*, Los Alamos National Laboratory, NM, U.S.A.
8. Chang PC, Flatau A, Liu SC. Review paper: health monitoring of civil infrastructure. *Structural Health Monitoring* 2003; **2**(3):257–267. DOI: 10.1177/1475921703036169.
9. Carden EP, Fanning P. Vibration based condition monitoring: a review. *Structural Health Monitoring* 2004; **3**(4):355–377. DOI: 10.1177/1475921704047500.
10. Chang PC, Liu SC. Recent research in nondestructive evaluation of civil infrastructures. *Journal of Materials in Civil Engineering* 2003; **15**:298–304. DOI: 10.1061/(ASCE)0899-1561(2003)15:3(298).
11. Ma T-W, Yang HT, Chang C-C. Structural damage diagnosis and assessment under seismic excitations. *Journal of Engineering Mechanics* (ASCE) 2005; **131**(10):1036–1045. DOI: 10.1061/(ASCE)0733-9399(2005)131:10(1036).
12. Sebastijanovic N, Ma T, Yang HTY. Structural damage detection and assessment using acceleration feedback. *Proceedings of SPIE* 2006; **6174**:61742L. DOI: 10.1117/12.659121.
13. Wrobleski MS, Yang HTY. Identification of simplified models using adaptive control techniques. *Journal of Structural Engineering* (ASCE) 2003; **129**(7):989–997. DOI: 10.1061/(ASCE)0733-9445(2003)129:7(989).
14. Han X, Favro LD, Ouyang Z, Thomas RL. Thermosonics: detecting cracks and adhesion defects using ultrasonic excitation and infrared imaging. *The Journal of Adhesion* 2001; **76**(2):151–162. DOI: 10.1080/00218460108029622.
15. Favro LD, Thomas RL, Han X, Ouyang Z, Newaz G, Gentile D. Sonic infrared imaging of fatigue cracks. *International Journal of Fatigue* 2001; **23**:471–476. DOI: 10.1016/S0142-1123(01)00151-7.
16. Han X, Favro LD, Thomas RL. Recent developments in sonic IR imaging. *AIP Conference Proceedings* 2003; **657**(1):500–504. DOI: 10.1063/1.1570177.
17. Han X, Islam MS, Newaz G, Favro LD, Thomas RL. Finite element modeling of the heating of cracks during sonic infrared imaging. *Journal of Applied Physics* 2006; **99**(7):074905. DOI: 10.1063/1.2189023.
18. Sebastijanovic N, Yang HTY, Ma T-W. Detection of changes in global structural stiffness coefficients using acceleration feedback. *Journal of Engineering Mechanics* (ASCE) 2010; **136**(9):1187–1191. DOI: 10.1061/(ASCE)EM.1943-7889.0000159.
19. Craig Jr RR. *Structural Dynamics*. Wiley: New York, 1981.
20. Biggs JM. *Introduction to Structural Dynamics*. McGraw-Hill: New York, 1964.
21. Spencer Jr BF, Christenson RE, Dyke SJ. Next generation benchmark control problem for seismically excited buildings. *Proceedings of the 2nd World Conference on Structural Control*, Kyoto, Japan, 1998.
22. Chen WF, Goto Y, Liew JYR. *Stability Design of Semi-Rigid Frames*. Wiley-Interscience: New York, 1995.
23. Bjorhovde R, Colson A, Brozzetti J. Classification system for beam-to-column connections. *Journal of Structural Engineering* 1990; **116**(11):3059–3076. DOI: 10.1061/(ASCE)0733-9445(1990)116:11(3059).
24. Li GQ, Li JJ. *Advanced Analysis and Design of Steel Frames*. Wiley: New York, 2007.
25. Lui EM, Chen W. Behavior of braced and unbraced semi-rigid frames. *International Journal of Solids and Structures* 1988; **24**(9):893–913. DOI: 10.1016/0020-7683(88)90040-6.
26. Yu CH, Shanmugam NE. Stability of semi-rigid space frames. *Composite Structures* 1988; **28**(1):85–91. DOI: 10.1016/0045-7949(88)90095-8.

27. Ho WMG, Chan SL. Semibifurcation and bifurcation analysis of flexibly connected steel frames. *Journal of Structural Engineering* 1991; **117**(8):2299–2319. DOI: 10.1061/(ASCE)0733-9445(1991)117:8(2299).
28. Wald F. Sensitivity of semi-rigid frames to initial imperfections. *3rd Stability Colloquium*, Budapest, Hungary, vol. 2, 1990; 305–311.
29. Sinha JK, Friswell MI, Edwards S. Simplified models for the location of cracks in beam structures using measured vibration data. *Journal of Sound and Vibration* 2002; **251**(1):13–38. DOI: 10.1006/jsvi.2001.3978.
30. Christides S, Barr ADS. One-dimensional theory of cracked Bernoulli-Euler beams. *International Journal of Mechanical Sciences* 1984; **26**(11–12):639–648. DOI: 10.1016/0020-7403(84)90017-1.
31. Chehil D, Jategaonkar R. Determination of natural frequencies of a beam with varying section properties. *Journal of Sound and Vibration* 1987; **115**(3):423–436.